DOI: 10.1021/ma9003067

Macromolecules
ARTICLE

Optimizing End-Labeled Free-Solution Electrophoresis by Increasing the Hydrodynamic Friction of the Drag Tag

Kai Grass,*,† Christian Holm,*,†,‡ and Gary W. Slater*,§

†*Frankfurt Institute for Advanced Studies, Goethe University, Ruth-Moufang-Strasse 1, D-60438 Frankfurt am Main, Germany,* ‡*Institute for Computational Physics, University of Stuttgart, Pfaffenwaldring 27, D-70569 Stuttgart, Germany, and* §*Department of Physics, University of Ottawa, 150 Louis-Pasteur, Ottawa, Ontario K1N 6N5, Canada*

Received February 10, 2009; Revised Manuscript Received May 12, 2009

ABSTRACT: We study the electrophoretic separation of polyelectrolytes of varying lengths by means of end-labeled free-solution electrophoresis (ELFSE). A coarse-grained molecular dynamics simulation model, using full electrostatic interactions and a mesoscopic Lattice Boltzmann fluid to account for hydrodynamic interactions, is used to characterize the drag coefficients of different label types: linear and branched polymeric labels as well as transiently bound micelles. It is specifically shown that the label's drag coefficient is determined by its hydrodynamic size and that the drag per label monomer is largest for linear labels. However, the addition of side chains to a linear label offers the possibility to increase the hydrodynamic size, and therefore the label efficiency, without having to increase the linear length of the label, thereby simplifying synthesis. The third class of labels investigated, transiently bound micelles, seems very promising for the usage in ELFSE, as they provide a significant higher hydrodynamic drag than the other label types. The results are compared to theoretical predictions, and we investigate how the efficiency of the ELFSE method can be improved by using smartly designed drag tags.

Introduction

As known from experiments and theory,[1−6] the free-solution mobility of a flexible polyelectrolyte chain does not depend on the chain length N (number of monomers) anymore if the chain is longer than a certain length N_{FD}. The regime where $N > N_{FD}$ is called free-draining regime. In this regime, the counterions influence the intermonomer hydrodynamic interactions and allow the fluid to drain through the polyelectrolyte coil. The effective friction Γ_{eff} becomes linear in the chain length, as does the effective charge Q_{eff} for longer chains, which leads to a constant, length-independent mobility

$$\mu_0 = \frac{Q_{eff}}{\Gamma_{eff}} \tag{1}$$

It was shown that attaching a suitable uncharged molecule to an electrophoresis target can restore the size-dependent mobility and overcome the free-draining property of long polyelectrolyte chains.[7−9] This method, which is known as *end-labeled free-solution electrophoresis* (ELFSE), is based on the alteration of the charge-to-friction ratio of the polyelectrolyte molecules by an uncharged drag label.

The effect of the label can be compared to that of a parachute attached to a moving object. The additional friction provided by the parachute slows the object down. This effect is stronger for smaller molecules with a lower effective friction and smaller charge to pull the drag tag, as the ratio between charge and friction is changed more drastically than for larger molecules.

Since the method's introduction, finding suitable labels that provide a high hydrodynamic drag has been a major concern in this field.[10−12] A larger hydrodynamic drag enables the separation of longer chain fragments, as the length dependence of the electrophoretic mobility decreases with increasing polyelectrolyte length. When the additional friction provided by the drag tag becomes negligible against the intrinsic effective friction of the polyelectrolyte, the chain becomes essentially free-draining again. Experimentally relevant is that the mobility of long polyelectrolyte chains should differ by a factor large enough to allow for accurately separating them, although their lengths only vary by a single monomer. The maximum chain length resolvable in this way is called the *read length*.

In general, the drag labels can be chosen from a wide range of molecules but they have to fulfill certain requirements, such as being water-soluble at experimental conditions, having a unique attachment mechanism to the polyelectrolyte and showing minimal interaction with the walls of the capillary. The read length is optimized by choosing a large molecule that imposes a high frictional drag. However, to fulfill resolution requirements, the labels must remain perfectly monodisperse since polydispersity will effectively be like an additional source of diffusion that would broaden the peaks.

As it poses an experimental challenge to produce large, monodisperse linear polymer labels, two recently proposed alternatives seem promising. Haynes et al.[13] proposed to use branched polymers with well-defined architectures. A first theoretical study on this method[14] verified the approach and concluded that, even though a branched polymer is more compact and thus provides a smaller hydrodynamic friction for a given molecular weight than a linear polymer, this drawback is offset by the monodispersity of the branched labels created by assembling shorter linear chains. Grosser et al.[15−17] introduced nonionic surfactant micelles as drag labels with very large hydrodynamic friction. The inherent polydispersity of the micelles is overcome by using a PNA amphiphile that only provides a transient binding between the DNA fragments to be separated and the micelles.

*Corresponding author. E-mail: grass@fias.uni-frankfurt.de.

 Published on Web 06/19/2009

Each fragment attaches to a different micelle every couple of seconds, which results in an averaging procedure over the course of the elution time that remedies the need for perfect monodispersity.

The theoretical description of the methods discussed above is not complete and furthermore predicts behaviors that are difficult to test experimentally, such as end of chain effects, the hydrodynamic deformation of the label in high fields, or the steric segregation between the label and the chain. Since it is not possible to visualize DNA-label molecules in the lab, computer simulations can support the understanding of the real physics as long as they include hydrodynamic interactions between polyelectrolyte, label and solvent, as well as account for the influence of the electrostatic interaction between the polyelectrolytes and its surrounding counterions. Of course, it is beyond the scope of this article to cover all previous predictions.[12,14,18−21] However, we will demonstrate that it is possible to study these factors and that the standard theory appears to be sufficient for the cases treated here. More cases will be studied in future papers.

Since the ELFSE method overcomes the main drawback of ordinary gel electrophoresis, the long separation time due to the slow down by the applied gel matrix, it is a promising method on the way to faster sequencing methods and, as such, of especial interest to the community. Recently, several alternative free-solution methods were developed that likewise might lead to significantly advanced electrophoretic separation.[22−25]

In this paper we will use coarse-grained MD simulations to study the electrophoretic separation of fully flexible polyelectrolytes of varying lengths by end-labeling. After introducing the simulation model, we confirm that the free-draining behavior is correctly reproduced and test the standard theory for ELFSE by attaching an uncharged linear label. We then introduce branches to the drag label and test the predictions made by.[13,14] From the branched label, we will go to micellar targets and analyze the method proposed by.[15,16] We establish a relation between the average size of the micelle and its drag value. Our concluding remarks point out the efficiency of the ELFSE method and show the benefit of the different labeling methods.

Theory

The theory for end-labeled free-solution electrophoresis is based on the interplay between hydrodynamic and electrostatic forces, and it takes into account the stress that builds along the chain backbone. In general, it is assumed that the electrostatic and frictional forces do not deform the hybrid molecule's random coil conformation nor its cloud of counterions. Because of these assumptions, the theory used here is valid for low velocities and weak electric fields.

Neglecting molecular end effects, the electrophoretic mobility $\mu = v/E$ of the polyelectrolyte with an attached linear drag tag can be described in terms of the effective friction of the polyelectrolyte Γ_{PE}, its effective charge Q_{PE}, and the hydrodynamic friction of the attached label Γ_L:

$$\mu = \frac{Q_{PE}}{\Gamma_{PE} + \Gamma_L} = \mu_0 \frac{1}{1 + \Gamma_L/\Gamma_{PE}} \tag{2}$$

where μ_0 is the length-independent free solution mobility without drag tag.

Equation 2 shows the importance of the ratio between Γ_{PE} and Γ_L. The electrophoretic mobility μ is a function of N for a fixed Γ_L as long as Γ_{PE} changes with N and the ratio between Γ_L and Γ_{PE} remains non-negligible.

Since the electrophoretic friction coefficient Γ_{PE} grows linear with the length of the polyelectrolyte for long chains, as shown in a previous publication,[26] eq 2 can be reformulated as follows:

$$\mu = \mu_0 \frac{1}{1 + \alpha_L/N} \tag{3}$$

with a constant drag coefficient

$$\alpha_L = \frac{\Gamma_L}{\Gamma_{PE}/N} \tag{4}$$

Here the ratio Γ_{PE}/N is the friction per monomer of the polyelectrolyte. The chemistry and temperature dependent α_L is a measure for the difference in hydrodynamic properties between the polyelectrolyte and the label and represents the number of polyelectrolyte monomers that provide a hydrodynamic friction equal to that of the label.[8,12,18,19,27]

In order to characterize the effectiveness of an arbitrary (not necessarily linear) label for size separation, eq 3 has been used to define this specific label property from the measured mobilities:

$$\alpha_L = N\left(\frac{\mu_0}{\mu} - 1\right) \tag{5}$$

where α_L is conveniently determined as the slope when plotting μ_0/μ vs $1/N_{PE}$:

$$\frac{\mu_0}{\mu} = 1 + \alpha_L/N \tag{6}$$

Simulation Model

We employ coarse-grained molecular dynamics (MD) simulations using the ESPResSo package[28] to study the electrophoretic separation of fully charged linear flexible polyelectrolytes by end-labeled free-solution electrophoresis. The polyelectrolytes are modeled by a totally flexible bead−spring model as a set of spheres that represent the N individual monomers which are connected to each other by finitely extensible nonlinear elastic (FENE) bonds:[29]

$$U_{FENE}(r) = \frac{1}{2}kr^2 \ln\left(1 - \left(\frac{r}{R}\right)^2\right)$$

with stiffness $k = 30\varepsilon_0$, maximum extension $R = 1.5\sigma_0$, and r being the distance between the interacting monomers. Additionally, a truncated Lennard-Jones or WCA potential is used for excluded volume interactions:[30]

$$U_{LJ}(r) = \varepsilon_0\left(\left(\frac{\sigma}{r}\right)^{12} - \left(\frac{\sigma}{r}\right)^{6} + \frac{1}{4}\right)$$

with the cutoff being $r_{cut} = 2^{1/6}\sigma$, at which $U_{LJ}(r) = 0$.

The parameters ε_0 and σ_0 define the energy and length scales of the simulations. We use $\varepsilon_0 = k_BT$; i.e., the energy of the system is expressed in terms of the thermal energy. The length scale σ_0 defines the size of the monomers. We set $\sigma_0 = 4.7$ Å, which with the average bond length along the PE chain being $0.91\sigma_0$ represents a linear monomer distance of ∼4.3 Å, the spacing of single-stranded DNA. Different polyelectrolytes can be mapped by changing σ_0. Unless mentioned otherwise, all observables are expressed in terms of the simulation units σ_0 and ε_0, which we will not use explicitly from now on.

Besides the dissociated counterions the system also contains additional monovalent salt. The counterions and the salt ions are modeled as charged spheres using the same WCA potential giving all particles in the system the same size.

All chain monomers carry a negative electric charge $q = -1e_0$, where e_0 is the elementary charge. For charge neutrality,

N monovalent counterions of charge $+le_0$ are added. Additional monovalent salt is added to the simulation. Full electrostatic interactions are calculated with the P3M algorithm using the implementation of ref 31. The Bjerrum length $l_B = e_0^2/4\pi\varepsilon k_B T = 1.5$ in simulation units corresponds to 7.1 Å, the Bjerrum length in water at room temperature. This means that the effect of the surrounding water is modeled implicitly by simply employing the dielectric properties of water, using a relative dielectric constant of $\varepsilon_r \approx 80$. The applied external field $E = 0.1$ is represented by a constant force, acting on all charged particles. The field strength is chosen to be sufficiently small in order to not influence chain conformations or counterion distributions.

The coarse-grained molecular dynamics model used in this article is extended by the inclusion of the three drag-tag labels investigated, as shown in Figure 1. The linear labels use the same flexible bead−spring model as the polyelectrolytes but are uncharged. For the study of branched labels, flexible side chains of well-defined length are added to the linear label. The third kind of label, micellar drag tags, is represented by a sphere of given radius whose surface is modeled by many small WCA spheres that are connected with each other by a network of FENE springs. The number of small spheres is defined by the radius of the large sphere to be modeled. This model has been successfully used to study colloidal electrophoresis.[32−34]

We include hydrodynamics using a lattice Boltzmann (LB) algorithm[35] that is frictionally coupled to the MD simulations via an algorithm introduced by Ahlrichs et al.[36] The mesoscopic LB fluid is described by a velocity field generated by discrete momentum distributions on a spatial grid, rather than explicit fluid particles. We use an implementation of the D3Q19 model with a kinematic viscosity $\nu = 1.0$ and a fluid density $\rho = 1.0$.[37] The resulting fluid has a dynamic viscosity $\eta = \rho\nu = 1.0$. The space is discretized by a grid with spacing $a = 1.0$. The fluid is coupled to the particles by a frictional coupling with bare friction parameter $\Gamma_{bare} = 20.0$. The value of Γ_{bare} was chosen in such a way that the single particle diffusion coefficient D_0 within the LB fluid corresponds to that obtained in simulations using an explicit fluid consisting of soft WCA spheres.[38] Random fluctuations for particles and fluid act as a thermostat. The interaction between particles and fluid conserve total momentum and are proved to yield correct long-range hydrodynamic interaction between individual particles.

The simulations are carried out under periodic boundary conditions in a cubic simulation box. We investigate the behavior of polyelectrolyte chains varying from $N = 20$ to $N = 60$ monomers. The size L of the box is varied to realize a constant monomer density of $n_{PE} = 10^{-3}$, which corresponds to a concentration $c_{PE} = 16$ mM. The same concentration is used for the additional salt, resulting in a Debye length of $\lambda_D \approx 4.2$. A MD time step $\tau_{MD} = 0.01$ and a LB time step $\tau_{LB} = 0.05$ are used. After equilibration of 10^6 steps, 10^7 steps are used for generating the data. The time series are analyzed using autocorrelation functions to estimate the statistical errors as detailed in ref 39. Error bars of the order of the symbol size or smaller are omitted in the figures.

The electrophoretic mobility is obtained by applying a constant electric field of reduced field strength $E = 0.1$ that acts on all charged particles. The mobility is then given by direct measurement of the center of mass velocity v of the chain:

$$\mu = \frac{v}{E} \tag{7}$$

Before applying this method, it was ensured that the applied electric field strength E is small enough not to distort chain conformations or counterion distributions. Therefore, the system is in the linear response regime; i.e., the measured mobility does not depend on the magnitude of the electric field.

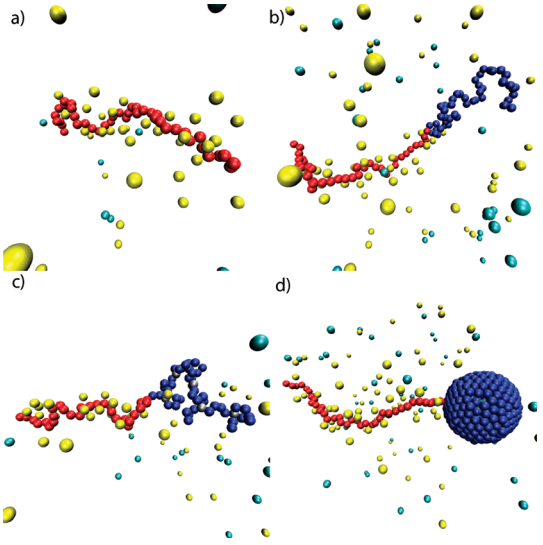

Figure 1. (a) Polyelectrolyte with surrounding counterions and co-ions, (b) with a linear drag tag, (c) with a branched polymeric drag tag, and (d) with a micellar drag tag.

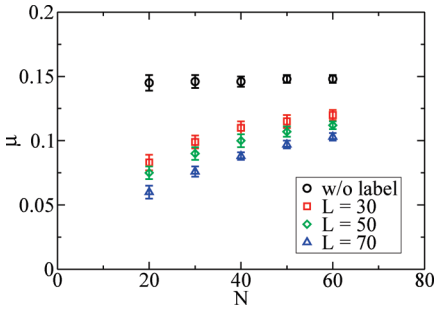

Figure 2. Free-solution electrophoretic mobility without label (black circles) shows no dependence on the chain length N. The free-draining mobility is $\mu_0 = 0.147 \pm 0.002$. The attachment of linear drag tags to the end of the polyelectrolyte chains reduces the mobility and restores a N-dependent behavior. The label length L is varied from 30 to 70 monomers, with the largest label resulting in the strongest slowdown.

Up to 10 independent simulations are carried out for each data point, taking between 1 day and 2 weeks on a single standard CPU (Dual Core AMD Opteron Processor 270) depending on the chain length N and the type of label investigated.

Linear Drag Tags

In this section, the simulation model is applied to the electrophoresis of polyelectrolyte chains with an attached linear polymeric drag tag. The electrophoretic mobility for polyelectrolyte chains is determined with and without different labels, and the results are compared to the theoretical predictions. We also examine how the effective friction of the drag tag is influenced by the intrinsic stiffness and the salt concentration in the solution.

Testing the Standard ELFSE Theory. First, the free-solution electrophoretic mobility without an attached drag tag, μ_0, is determined, as shown in Figure 2. The measured mobility does not depend on the chain length, as expected for longer free-draining polyelectrolyte chains. The average mobility is determined to be

$$\mu_0 = 0.147 \pm 0.002 \tag{8}$$

Additionally, in Figure 2, the mobilities with attached drag tags ranging from $L = 30$ to $L = 70$ monomers are measured, and it is confirmed that a length dependence is

achieved and that the difference in mobilities, i.e., the selectivity of the separation, is better the longer the attached label is. Equation 6 is used to calculate the hydrodynamic drag coefficients as shown in Figure 3, resulting in values from $\alpha_L = 13.5 \pm 0.4$ for $L = 30$ to $\alpha_L = 25.7 \pm 0.6$ for $L = 70$.

In the following, an expression for α_L based on the hydrodynamic size and shape of the label is developed. The hydrodynamic friction Γ_L of the uncharged label is related to the hydrodynamic radius R_h by means of the Stokes relation:

$$\Gamma_L = 6\pi\eta R_{h,L} \tag{9}$$

The hydrodynamic radius of the label is given by

$$\langle \frac{1}{R_{h,L}} \rangle = \frac{1}{N} \sum_{i \neq j} \langle \frac{1}{\| \vec{r}_i - \vec{r}_j \|} \rangle \tag{10}$$

Here, $\vec{r}_i$ iterates the positions of the label monomers and $\vec{r}_{cm}$ the center of mass of the label. The angular brackets $\langle ... \rangle$ indicate an ensemble average.

As in the previous section, the effective electrophoretic friction of the polyelectrolyte is expressed in terms of the free-solution mobility μ_0 and the effective charge Q_{eff}:

$$\Gamma_{PE} = Q_{eff}/\mu_0 \tag{11}$$

Using the Manning prediction $Q_{eff} = (1/\xi)N$ for the effective charge,[40] where the Manning condensation parameter $\xi = l_B/b$ is a measure for the strength of the electrostatic potential of the polyelectrolyte, finally yields

$$\alpha_L = \mu_0 \xi 6\pi\eta R_{h,L} \tag{12}$$

With the system parameter used here, $\xi = 1.63$, one obtains

$$\alpha_L = (4.5 \pm 0.1) R_{h,L} \tag{13}$$

Equation 12 will be shown to be valid for linear labels whose size is not exceeding the Debye length λ_D. When the label size becomes larger, the friction of the label is not anymore directly related to the hydrodynamic radius, as the salt ions that penetrate the polymer coil influence the intermonomer hydrodynamic interactions and limit them to the electrostatic screening length. As for the polyelectrolyte itself, this screening length is of the order of the Debye length.

For linear labels larger than the Debye length, McCormick et al. introduced a relation for the hydrodynamic drag coefficient, with which α_L can be determined from the size of the polyelectrolyte and label monomers, b_{PE} and b_L, and the corresponding Kuhn lengths, $b_{k,PE}$ and $b_{k,L}$, which describe the stiffness of the chains:[18]

$$\alpha_L = \frac{b_L b_{k,L}}{b_{PE} b_{k,PE}} L \tag{14}$$

The derivation of eq 14 assumes that the polyelectrolyte and the label can be represented by a series of hydrodynamically equivalent entities, called "blobs" as shown in Figure 4. The number and the size of these blobs depend on the bond length and flexibility of the chains, resulting in the presented relation for α_L.

The total effective friction of the polyelectrolyte-label compound with the surrounding solvent is linear in the total number of hydrodynamically equivalent monomers given by

$$N = N_{PE} + \alpha N_L \tag{15}$$

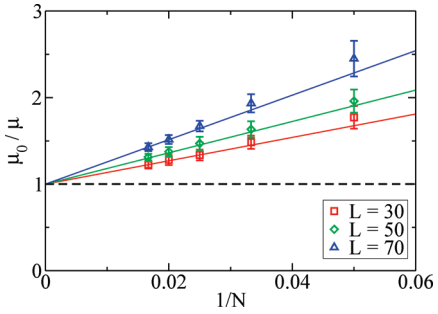

Figure 3. Hydrodynamic drag coefficient α_L is given by the slope of the curve. For the linear labels, α_L ranges from 13.5 ± 0.4 to 25.7 ± 0.6.

This is true for long polyelectrolytes in the free-draining regime, where the size of the compound is larger than the Debye length λ_D, since the hydrodynamic interactions between the individual monomers are screened on this length scale, as shown in a prior study on free-solution electrophoresis.[26,41]

Thus, the hydrodynamic drag α_L can be directly calculated from the persistence lengths of the polyelectrolyte and of the label using eq 14. Here, $l_{p,PE}$ and $l_{p,L}$ are calculated from the bond correlation function:[42]

$$l_p = \frac{1}{2b} \sum_{i=0}^{N/2} \langle \vec{b}_{N/2} \cdot \vec{b}_{N/2+i} + \vec{b}_{N/2} \cdot \vec{b}_{N/2-i} \rangle \tag{16}$$

where $\vec{b}_i$ is the ith bond vector and b is the average bond length. The angular brackets $\langle ... \rangle$ denote an ensemble average (for a discussion about different ways to determine the persistence length in computer simulations please refer to ref 43).

Under the chosen conditions, the persistence length of the polyelectrolyte is found to be

$$l_{p,PE} = 5.1 \pm 0.3$$

and the label's one

$$l_{p,L} = 1.9 \pm 0.1$$

The difference between these two values is due to the electrostatic repulsion between the monomers of the polyelectrolyte. In our model, all monomers have the same size, so that eq 14 is reduced to

$$\alpha_L = \frac{l_{p,L}}{l_{p,PE}} L = (0.37 \pm 0.03) L \tag{17}$$

The comparison between the measured drag coefficient and the theoretical prediction in Figure 5 shows an agreement for the respective regimes of validity. The agreement between theory and experiments has been shown before.[10,18,44] For labels with a hydrodynamic size smaller than the Debye length, i.e., $R_h < \lambda_D$, eq 12 gives the correct prediction for the drag coefficient α_L. Longer labels, however, can no longer be seen as a single polymer coil with a hydrodynamic size R_h, but instead the blob picture described by eq 14 has to be used. This prediction is only valid when the hydrodynamic size becomes larger than the Debye length. For $R_h \approx \lambda_D$ the expected crossover between these regimes is observed.

It remains to be emphasized that, by determining α_L from the measurements of the persistence lengths and the hydrodynamic radius, there is *no free* fitting parameter and the *quantitative* agreement in Figure 5 is noteworthy.

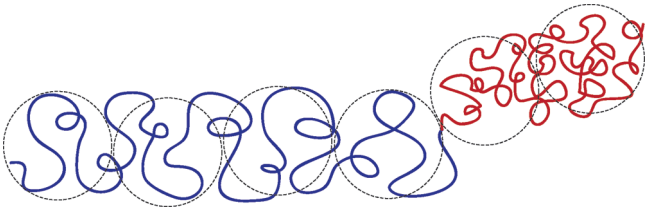

Figure 4. Schematic representation of the "blob" picture used to derive eq 14.

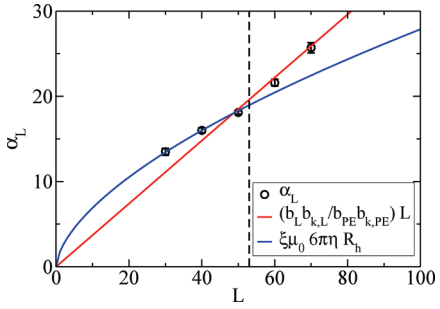

Figure 5. Hydrodynamic drag coefficient α_L for the linear label is compared to the theoretical predictions of eqs 12 and 14. Both predictions are valid in different regimes with the division being $R_h \approx \lambda_D$ indicated by the vertical dashed line. Note that neither theory has a free fitting parameter used to achieve the quantitative agreement with the simulation data.

Increasing the Hydrodynamic Drag Coefficient. In Figure 5, it is shown that the total drag coefficient α_L for linear labels can be increased by using longer labels and that beyond the Debye length the increase is linear with the length L of the label. Unfortunately, the experimental requirement of strict monodispersity of the label limits the size of linear polymeric labels that can be synthesized and prepared. In this section, it will be shown how one can influence the total drag coefficient also by modifying the relative stiffness of the polyelectrolyte and drag-tag chains.

Increasing the Label Stiffness. Equation 14 shows the dependence of α_L on the persistence lengths of polyelectrolyte and label. Therefore, α_L can be increased by either increasing the persistence of the label or decreasing the persistence of the polyelectrolyte. Both ways will be investigated in this subsection.

First, an additional harmonic bond angle potential

$$U_{BA} = k_{BA}(\phi - \phi_0)^2 \qquad (18)$$

is added to the interaction between the label monomers, where ϕ is the angle between two consecutive bonds. Here, $k_{BA} = 30$ and $\phi_0 = 0$ are chosen.

The bond angle potential increases the hydrodynamic radius of the 30 monomer label from $R_{h,L} = 3.00 \pm 0.05$ to

$$R_{h,L} = 5.25 \pm 0.05$$

and thus puts the label size into the regime where the blob picture is valid. The increased stiffness doubles the persistence length of the label from $l_{p,L} = 1.9 \pm 0.1$ to

$$l_{p,L} = 4.0 \pm 0.1$$

which yields an increased drag coefficient according to eq 14 of

$$\alpha_L = (0.79 \pm 0.04)L \approx 23.7$$

Figure 6 compares the theoretical predicted slowdown of the stiffer 30 monomeric label to the measured mobilities.

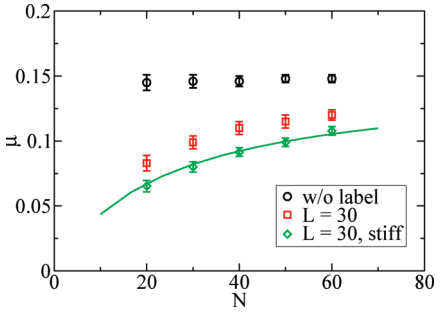

Figure 6. Hydrodynamic drag coefficient of a stiff linear label is higher than that of a fully flexible label with the same length. The slowdown of the stiff label is correctly predicted by eq 14 (solid line).

As before, an excellent agreement to the theory is found for the investigated label lengths. Please note that there is no fitting parameter here.

Reducing the Polyelectrolyte Stiffness. In practice, it is not easy to increase the stiffness of the drag tag in order to to increase α_L since this implies changing the chemistry of the label. However, the value of α_L is a relative measure of the stiffness of the two components of the hybrid polyelectrolyte-label molecule (see eq 14). Therefore, an increase of α_L can also be achieved if we reduce the stiffness of the polyelectrolyte. The persistence length of a polyelectrolyte can be reduced very effectively by increasing the ionic strength of the buffer: this increases the screening of the electrostatic repulsive interactions that stiffen the backbone of the charged polymer. In this subsection, we investigate the effect of changing the concentration of salt from $c_S = 16$ mM to $c_S = 1$ M, which reduces the Debye length from $\lambda_D \approx 4.2$ to $\lambda_D \approx 0.65$.

The increased electrostatic screening reduces the extension of the polyelectrolyte chain and reduces the contribution of electrostatics to the persistence length, which is determined to be

$$l_{p,PE} = 3.8 \pm 0.2$$

whereas the label persistence is unaffected. Thus, one predicts a hydrodynamic drag coefficient of

$$\alpha_L = (0.50 \pm 0.04)L$$

using eq 14, instead of

$$\alpha_L = (0.37 \pm 0.03)L$$

for the previous salt concentration (see eq 17).

The change in electrophoretic mobilities for labels of lengths $L = 20$ and $L = 40$ can be seen in Figure 7. Please note that the free-draining mobility μ_0 also changes due to the fact that the additional salt also increases the screening of the polyelectrolyte charge, thus reducing the net force from the external field:

$$\mu_0 = 0.113 \pm 0.002$$

The reduction in the absolute mobility μ_0 together with the increase of the diffusion coefficient due to the more compact conformation of the molecules at higher salt concentrations negatively affect the size selectivity as can be seen when evaluating the resolution factor R as defined by McCormick et al.[18] If we keep the polyelectrolyte length N, the label length L, the electric field strength E and the elution distance constant then one obtains for a given α_L a resolution factor

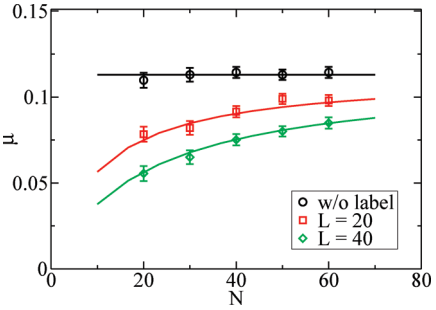

Figure 7. In the presence of 1 M additional salt, the persistence length of polyelectrolyte is reduced, changing the relative hydrodynamic drag α_L of the label. The observed mobility of the polyelectrolyte molecules for two linear labels of length 20 and 40 are compared to the prediction using eq 14.

R that only depends on the diffusion coefficient D_0 and the free-draining mobility μ_0:

$$R \sim \sqrt{D_0/\mu_0}$$

The way the resolution factor is defined a higher value indicates a lower size selectivity, and thus the size selectivity is decreased if the relative drag of the label is increased by increasing the salt concentration. Consequently, an increased hydrodynamic drag coefficient is less effective when achieved by adding additional salt.

Branched Drag Tags

In this section, we will investigate the use of branched labels as a possible way to synthesize more efficient ELFSE drag tags. First, the results obtained in a recent experimental study by Haynes et al. are briefly reviewed.[13] The study compared a linear polypeptide drag tag with 30 repeat units to two branched drag tags, each with 5 side chains spaced evenly along a 30-unit-long backbone. The two different branched labels had 4 and 8 monomer long side chains. The drag coefficients α_L were obtained by measuring the mobility of two different DNA fragments of 20 and 30 bases in length. It was found that the value of α_L increases roughly linearly with the total molecular weight of the branched label.

This astonishing observation was theoretically analyzed by Nedelcu et al.[14] It was shown that the drag coefficient is directly related to the hydrodynamic radius (as one would expect from the blob picture) and that the linear dependence on molecular weight is only approximately true in the limit of short side chains.

As a matter of fact, the drag provided by a linear label is always higher than that provided by a branched label of the same molecular weight. The reason for this is that, with a fixed length backbone, a branched polymer is essentially a compact star polymer with a smaller hydrodynamic size than the linear equivalent. Indeed, as the number of arms increases, the branched polymer becomes even more compact and less favorable for ELFSE.

Based on the observations, the following optimal design using branched polymeric labels for ELFSE was proposed: (I) side chains with length comparable to the distance between branching points or (II) two long branches located near the ends of the molecule's backbone.

Here, the focus will be on investigating the effect of the length of the side chains for a polymeric drag tag with a fixed backbone length. Similar to the structure of the label used by Haynes et al., the label has a backbone of $L = 30$ monomers, to which 5 side chains are attached evenly spaced along the backbone. The side-chain length is varied from 2 to 8 monomers, so that the total number of monomers in the label ranges from 40 to 70.

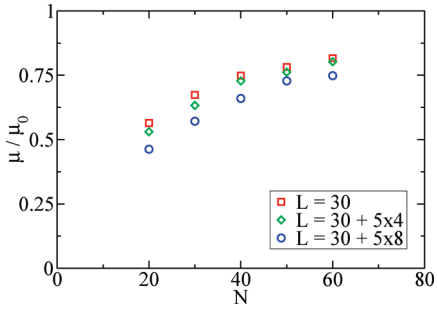

Figure 8. Reduced mobility μ/μ_0 for polyelectrolytes with an attached linear label with five side chains of length 4 and 8 shows a more pronounced slowdown than for the label without side chains.

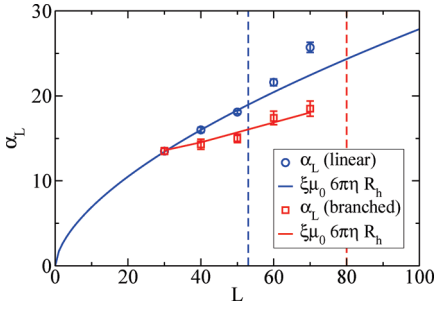

Figure 9. Hydrodynamic drag coefficient α_L of a branched polymeric label is compared to the previously determined drag of a linear label. L is the total number of monomers. As long as the hydrodynamic radius R_h of the label is smaller than the Debye length λ_D, the α_L is given by eq 12. The vertical lines indicate the number of monomers L for which $R_h(L) \approx \lambda_D$ obtained from simulations.

The backbone as well as the side chains of the branched label uses the fully flexible bead−spring model presented in the model description. The drag coefficient of the labels is determined by measuring the electrophoretic mobility of polyelectrolyte chains from $N = 20$ to $N = 60$.

Figure 8 shows the simulation results for a 30 monomeric label without side chains and with the tetra- and octamer side chains. To analyze the hydrodynamic drag of the branched labels in detail, α_L is determined according to eq 6. The obtained α_L values are compared to the corresponding value of a purely linear drag tag with the same number of monomers.

Figure 9 confirms the work by Nedelcu, showing that the label with the highest drag per monomer is the linear label. For the same number of monomers L, the hydrodynamic drag coefficient α_L of the linear label is higher than that of the branched one. But it also shows that the addition of side chains can be used to increase the hydrodynamic drag of the label. This is attributed to two effects: first, the hydrodynamic size of the label is increased as the side chains extend from the label. Of similar importance is the second effect, namely that the side chains stiffen the label due to steric repulsion with the backbone, increasing the overall persistence length and increasing the linear length of the backbone. In fact, this is the main contribution to the increase for the side chains of two and four monomers as we confirmed by measuring the change in persistence length of the backbone.

Interestingly, the drag coefficients obtained for the labels show a scaling with the hydrodynamic radius R_h, as given by eq 12. Since the polymer coil formed by the branched label is more compact, it is less penetrated by ions, and therefore, the prediction of eq 12 remains valid for a higher number of monomers compared to the linear label.

The experimentally observed linear scaling with L can be attributed to seemingly linear relationship between R_h and L,

but as Nedelcu et al. have shown before, this is only approximately true in the case of side chains smaller than or equal to the spacing along the backbone. The only relevant quantity in all cases is the hydrodynamic radius and its contribution to the hydrodynamic drag, as formulated in eq 12.

Although linear labels remain preferable as long as the pure hydrodynamic drag coefficient α_L per molecular weight is concerned, branched polymers offer practical advantages because of the possibility of synthesizing larger and somewhat stiffer monodisperse molecules in a simple, stepwise way.

Micellar Drag Tags

Recently, Grosser et al.[15,17] proposed another promising class of drag tags that in principle can provide very large hydrodynamic drag coefficients α_L. They used nonionic surfactant Triton X-100 micelles that attach to PNAA-taged (PNA amphiphile) DNA strands. The micelles are water-soluble and are created and destroyed on a time scale of milliseconds to seconds, forming a fairly monodisperse populations of structures with a tunable size and morphology. During the whole electrophoresis time, a single DNA strand attaches to a large number of different micelles. Of importance for the ELFSE application is the fact that this leads to an averaging effect between micelles of different sizes for the individual DNA strand, meaning the DNA can be though of as having a drag tag of fixed size $\langle R \rangle$, where $\langle R \rangle$ is the average micelle size. Only with this averaging, the natural polydispersity of the micelles is overcome and a measurement with a size resolution up to a couple of base pairs is possible.

As a free DNA strand quickly attaches to a new micelle, the DNA is bound to a micelle most of the electrophoresis time. Consequently, the transiently bound micelles provide about the same hydrodynamic drag as a covalently bound drag tag of similar size would provide. The reported α_L values range between 33 and 58 for a single micelle, depending on the micelle type and the PNAA molecule used for connecting to the DNA strand. Savard et al.[17] showed that dual tagging of the DNA, i.e., attaching a PNAA molecule to both ends of the DNA strand so that two micelles are transiently bound, can increase the hydrodynamic drag even further.

In this study, four different micelles with radius $R = 2$ to $R = 5$ are attached to polyelectrolyte chains of different lengths. Neither the attaching and detaching process nor the forming of the micelles themselves is modeled explicitly; only the hydrodynamic drag of a covalently bound spherical drag tag is investigated. The results by Grosser and Savard show that the polyelectrolyte is in fact attached to micelles for most of the time and only spends a small fraction of time without a drag tag. As the micelle size can be exactly chosen in simulations, the averaging procedure resulting from the attaching and detaching process does not need to be included.

Figure 10 shows that micellar drag tags can be successfully used for electrophoretic separation of polyelectrolyte chains. The values for α_L are obtained as before and compared to eq 12, which correctly predicts the observed behavior. With the chosen micelle radius of $R = 5$, drag coefficients up to $\alpha_L = 24.3$ are achieved.

The results show that the hydrodynamic drag is directly related to the size of the micelle, as can be seen in Figure 11. A linear increase with the radius is observed, as expected from Stokes theory. Again, eq 12 correctly predicts the drag coefficient, clearly indicating that only the hydrodynamic size of the drag tag is important, not the number of units it is made of or the weight associated with it.

The authors strongly believe that the use of micellar drag tags has great potential for the further advancement of end-labeled free-solution electrophoresis. Especially the tunable size makes them ideal candidates, as the drag coefficient can be optimized to the lengths of polyelectrolyte fragments to be analyzed. Currently, we are investigating the usability of cationic micelles as drag tags carrying positive charges, which create an additional force on the polyelectrolyte-label compound, possibly enhancing the size separation.

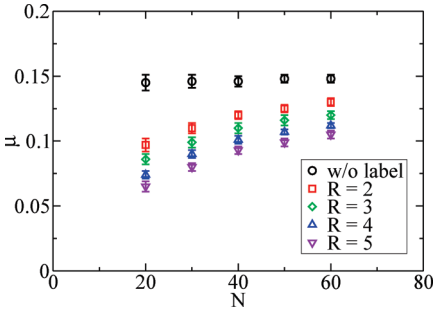

Figure 10. Electrophoretic mobility μ as a function of the polyelectrolyte length N becomes size dependent when a micellar drag tag is attached. The magnitude of the slowdown depends on the radius R of the micelle.

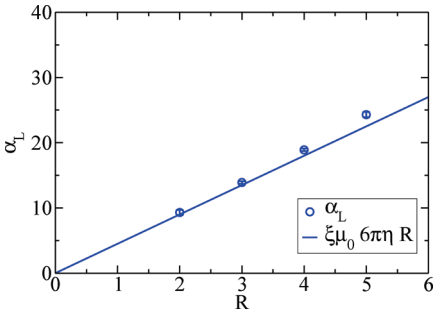

Figure 11. Effective hydrodynamic drag coefficient α_L of a micellar drag tag is directly proportional to its radius R. Equation 12 (the solid line) gives a very good prediction of the drag coefficient for all tested micelles.

Conclusion

In this paper, we have presented a detailed study of end-labeled free-solution electrophoresis (using various hydrodynamic drag tags) by coarse-grained molecular dynamics simulations. Linear, branched, and micellar drag tags were investigated. The simulations support the theoretical predictions and can be matched quantitatively to it. This enables the use of computer simulation as a tool to support the design of improved hydrodynamic drag tags usable for electrophoretic separation of polyelectrolytes in free solution.

It was specifically shown that the drag coefficient of the label is determined by its hydrodynamic size and not by its weight. The hydrodynamic drag per label monomer is largest for linear labels, but experimental restrictions in the synthesis of such labels and the monodispersity requirement limit their practical applicability.

The addition of side chains to a linear label offers the possibility to increase the hydrodynamic size without having to increase the linear length of the label. The synthesis process creates perfectly monodisperse labels. It was shown that the label efficiency is increased with the length of the side chains for the drag tag sizes studied in this work. In addition to increasing the lateral size of the drag tag, the side chains also increase the persistence of the backbone and thus contribute in two different ways to the increased hydrodynamic size. Especially the steric stiffening of the linear backbone is responsible for an initial increase of the drag coefficient with the total number of

monomers of the label, i.e., with the molecular weight. For longer side chains, the lateral contribution to the hydrodynamic radius becomes more important.

The third class of labels investigated seems very promising for the future of ELFSE. Transiently bound micelles provide a significantly higher hydrodynamic drag, as they can be prepared with a large hydrodynamic radius. Additionally, the time averaging by attaching to many different micelles over the electrophoresis time span helps to meet the monodispersity criteria. This study showed that the hydrodynamic drag is directly proportional to the hydrodynamic radius of the micelle. The efficiency of this method is, in principle, only limited by the size of labels that can be prepared.

Our results demonstrate convincingly that theory and computer models can support the experimental progress toward the design of novel improved drag tags, thereby extending the applicability of the ELFSE technique. The usability of charged drag tags is currently under investigation.

Acknowledgment. Funds from the Volkswagen foundation and the DAAD are gratefully acknowledged. All simulations were carried out on the compute cluster of the Center for Scientic computing at Goethe University Frankfurt. G.W.S. acknowledges the support from the Natural Science and Engineering Research Council of Canada.

References and Notes

(1) Stellwagen, E.; Lu, Y. J.; Stellwagen, N. C. *Biochemistry* **2003**, *42*, 11745–11750.
(2) Hoagland, D. A.; Arvanitidou, E.; Welch, C. *Macromolecules* **1999**, *32*, 6180–6190.
(3) Cottet, H.; Gareil, P.; Theodoly, O.; Williams, C. E. *Electrophoresis* **2000**, *21*, 3529–3540.
(4) Muthukumar, M. *Electrophoresis* **1996**, *17*, 1167–1172.
(5) Volkel, A. R.; Noolandi, J. *J. Chem. Phys.* **1995**, *102*, 5506–5511.
(6) Mohanty, U.; Stellwagen, N. C. *Biopolymers* **1999**, *49*, 209–214.
(7) Heller, C.; Slater, G. W.; Mayer, P.; Dovichi, N.; Pinto, D.; Viovy, J. L.; Drouin, G. *J. Chromatogr., A* **1998**, *806*, 113–121.
(8) Ren, H.; Karger, A. E.; Oaks, F.; Menchen, S.; Slater, G. W.; Drouin, G. *Electrophoresis* **1999**, *20*, 2501–2509.
(9) Desruisseaux, C.; Long, D.; Drouin, G.; Slater, G. W. *Macromolecules* **2001**, *34*, 44–52.
(10) Meagher, R. J.; Won, J.-I.; McCormick, L. C.; Nedelcu, S.; Bertrand, M. M.; Bertram, J. L.; Drouin, G.; Barron, A. E.; Slater, G. W. *Electrophoresis* **2005**, *26*, 331–350.
(11) Meagher, R. J.; McCormick, L. C.; Haynes, R. D.; Won, J. I.; Lin, J. S.; Slater, G. W.; Barron, A. E. *Electrophoresis* **2006**, *27*, 1702–1712.
(12) McCormick, L. C.; Slater, G. W. *Electrophoresis* **2005**, *26*, 1659–1667.
(13) Haynes, R. D.; Meagher, R. J.; Won, J. I.; Bogdan, F. M.; Barron, A. E. *Bioconjugate Chem.* **2005**, *16*, 929–938.
(14) Nedelcu, S.; Slater, G. W. *Electrophoresis* **2005**, *26*, 4003–4015.
(15) Grosser, S. T.; Savard, J. M.; Schneider, J. W. *Anal. Chem.* **2007**, *79*, 9513–9519.
(16) Savard, J. M.; Schneider, J. W. *Biotechnol. Bioeng.* **2007**, *97*, 367–376.
(17) Savard, J. M.; Grosser, S. T.; Schneider, J. W. *Electrophoresis* **2008**, *29*, 2779–2789.
(18) McCormick, L. C.; Slater, G. W.; Karger, A. E.; Vreeland, W. N.; Barron, A. E.; Desruisseaux, C.; Drouin, G. *J. Chromatogr., A* **2001**, *924*, 43–52.
(19) McCormick, L. C.; Slater, G. W. *Electrophoresis* **2007**, *28*, 674–682.
(20) McCormick, L. C.; Slater, G. W. *Electrophoresis* **2007**, *28*, 3837–3844.
(21) Nedelcu, S.; Meagher, R.; Barron, A.; Slater, G. W. *J. Chem. Phys.* **2007**, *126*, 175104.
(22) Viovy, J. L. *Rev. Mod. Phys.* **2000**, *72*, 813–872.
(23) Slater, G. W.; Guillouzic, S.; Gauthier, M. G.; Mercier, J. F.; Kenward, M.; McCormick, L. C.; Tessier, F. *Electrophoresis* **2002**, *23*, 3791–3816.
(24) Hu, S.; Dovichi, N. J. *Anal. Chem.* **2002**, *74*, 2833–2850.
(25) Kan, C. W.; Fredlake, C. P.; Doherty, E. A. S.; Barron, A. E. *Electrophoresis* **2004**, *25*, 3564–3588.
(26) Grass, K.; Holm, C. *J. Phys.: Condens. Matter* **2008**, *20*, 494217.
(27) Long, D.; Dobrynin, A. V.; Rubinstein, M.; Ajdari, A. *J. Chem. Phys.* **1998**, *108*, 1234–1244.
(28) Limbach, H. J.; Arnold, A.; Mann, B. A.; Holm, C. *Comput. Phys. Commun.* **2006**, *174*, 704–727.
(29) Soddemann, T.; Dünweg, B.; Kremer, K. *Eur. Phys. J. E* **2001**, *6*, 409.
(30) Weeks, J. D.; Chandler, D.; Andersen, H. C. *J. Chem. Phys.* **1971**, *54*, 5237.
(31) Deserno, M.; Holm, C. *J. Chem. Phys.* **1998**, *109*, 7678.
(32) Lobaskin, V.; Dünweg, B. *New J. Phys.* **2004**, *6*, 54.
(33) Lobaskin, V.; Dünweg, B.; Holm, C. *J. Phys.: Condens. Matter* **2004**, *16*, S4063–S4073.
(34) Lobaskin, V.; Dünweg, B.; Medebach, M.; Palberg, T.; Holm, C. *Phys. Rev. Lett.* **2007**, *98*, 176105.
(35) McNamara, G. R.; Zanetti, G. *Phys. Rev. Lett.* **1988**, *61*, 2332–2335.
(36) Ahlrichs, P.; Dünweg, B. *J. Chem. Phys.* **1999**, *111*, 8225–8239.
(37) Dünweg, B.; Schiller, U.; Ladd, A. *Phys. Rev. E* **2007**, *76*, 36704.
(38) Dünweg, B.; Kremer, K. *J. Chem. Phys.* **1993**, *99*, 6983–97.
(39) Wolff, U. *Comput. Phys. Commun.* **2004**, *156*, 143–153.
(40) Manning, G. S.; Ray, J. *J. Biomol. Struct. Dyn.* **1998**, *16*, 461–476.
(41) Grass, K.; Böhme, U.; Scheler, U.; Cottet, H.; Holm, C. *Phys. Rev. Lett.* **2008**, *100*, 096104.
(42) Hsiao, P.-Y. *Macromolecules* **2006**, *39*, 7125–7137.
(43) Ullner, M.; Woodward, C. E. *Macromolecules* **2002**, *35*, 1437–1445.
(44) Vreeland, W. N.; Desruisseaux, C.; Karger, A. E.; Drouin, G.; Slater, G W.; Barron, A. E. *Anal. Chem.* **2001**, *73*, 1795–1803.